

# Cellular Pharmacokinetics and Intracellular Activity of the Novel Peptide Deformylase Inhibitor GSK1322322 against *Staphylococcus aureus* Laboratory and Clinical Strains with Various Resistance Phenotypes: Studies with Human THP-1 Monocytes and J774 Murine Macrophages

Frédéric Peyrusson,<sup>a</sup> Deborah Butler,<sup>b</sup>  Paul M. Tulkens,<sup>a</sup>  Françoise Van Bambeke<sup>a</sup>

Pharmacologie cellulaire et moléculaire, Louvain Drug Research Institute, Université catholique de Louvain, Brussels, Belgium<sup>a</sup>; GlaxoSmithKline, Collegeville, Pennsylvania, USA<sup>b</sup>

GSK1322322 is a peptide deformylase inhibitor active against *Staphylococcus aureus* strains resistant to currently marketed antibiotics. Our aim was to assess the activity of GSK1322322 against intracellular *S. aureus* using an *in vitro* pharmacodynamic model and, in parallel, to examine its cellular pharmacokinetics and intracellular disposition. For intracellular activity analysis, we used an established model of human THP-1 monocytes and tested one fully susceptible *S. aureus* strain (ATCC 25923) and 8 clinical strains with resistance to oxacillin, vancomycin, daptomycin, macrolides, clindamycin, linezolid, or moxifloxacin. Uptake, accumulation, release, and subcellular distribution (cell fractionation) of [<sup>14</sup>C]GSK1322322 were examined in uninfected murine J774 macrophages and uninfected and infected THP-1 monocytes. GSK1322322 demonstrated a uniform activity against the intracellular forms of all *S. aureus* strains tested, disregarding their resistance phenotypes, with a maximal relative efficacy ( $E_{max}$ ) of a 0.5 to 1 log<sub>10</sub> CFU decrease compared to the original inoculum within 24 h and a static concentration ( $C_s$ ) close to its MIC in broth. Influx and efflux were very fast (<5 min to equilibrium), and accumulation was about 4-fold, with no or a minimal effect of the broad-spectrum eukaryotic efflux transporter inhibitors gemfibrozil and verapamil. GSK1322322 was recovered in the cell-soluble fraction and was dissociated from the main subcellular organelles and from bacteria (in infected cells). The results of this study show that GSK1322322, as a typical novel deformylase inhibitor, may act against intracellular forms of *S. aureus*. They also suggest that GSK1322322 has the ability to freely diffuse into and out of eukaryotic cells as well as within subcellular compartments.

The spread of multidrug-resistant *Staphylococcus aureus* strains in hospitalized patients and other individuals without health care-related risk factors raises alarming concerns in various countries and clinical settings due to the increasing likelihood of treatment failures and ensuing morbidity and mortality (1–3). In addition, the ability of *S. aureus* to sojourn and thrive intracellularly, well described in *in vitro* and *in vivo* models (4–7) and also documented in human infections, is considered to play a critical role in their persistent and recurrent character (8–10). Intracellular sheltering of *S. aureus*, indeed, leads to a considerable loss in antibacterial efficacy (defined as the ability of the antibiotic to decrease the intracellular bacterial load at the maximal achievable extracellular concentration), even for molecules that accumulate to large extents in eukaryotic cells (11). In this context, antibiotics acting on novel bacterial targets (and therefore potentially active against strains resistant to currently used antibiotics) and maintaining activity against intracellular forms of *S. aureus* are critically needed.

Peptide deformylase (PDF) is a metalloenzyme that removes the formyl group during eubacterial peptide elongation, playing a crucial role in protein maturation. PDF has been shown to be essential for bacterial growth and highly conserved in bacteria (12). Interestingly enough, PDF mutants that resist the action of PDF inhibitors show a severe fitness cost, substantial loss of pathogenicity, and a restricted ability to produce an invasive infection, all properties that may prevent them from being successful if emerging in the clinical arena (13). This makes PDF a desirable

novel target for antibiotic discovery and development. Thus, a large number of PDF inhibitors have been obtained over the past decade (14) by researchers who were partly inspired by studies of actinonin, a naturally occurring antibacterial that acts by inhibiting PDF (15). Among them, GSK1322322 (see chemical structure in Fig. 1) shows remarkably constant *in vitro* antibacterial activity against *S. aureus* strains with resistance to many currently marketed antibiotics (16). It is also the first molecule within this class that has progressed through phase II clinical trials as an oral and intravenous agent for the treatment of hospitalized patients with community-acquired bacterial pneumonia and acute bacterial skin and skin structure infections (17). The aims of the present

Received 7 April 2015 Returned for modification 20 June 2015

Accepted 4 July 2015

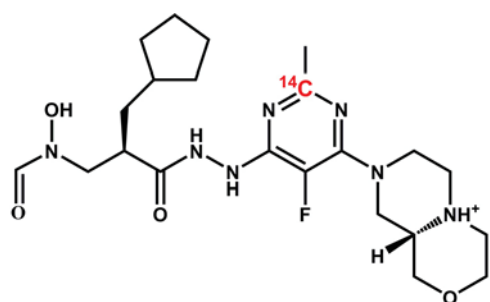
Accepted manuscript posted online 13 July 2015

Citation Peyrusson F, Butler D, Tulkens PM, Van Bambeke F. 2015. Cellular pharmacokinetics and intracellular activity of the novel peptide deformylase inhibitor GSK1322322 against *Staphylococcus aureus* laboratory and clinical strains with various resistance phenotypes: studies with human THP-1 monocytes and J774 murine macrophages. *Antimicrob Agents Chemother* 59:5747–5760. doi:10.1128/AAC.00827-15.

Address correspondence to Françoise Van Bambeke, francoise.vanbambeke@uclouvain.be.

Copyright © 2015, American Society for Microbiology. All Rights Reserved.

doi:10.1128/AAC.00827-15



(5*S*,9*aS*)-8-(6-(2-((*R*)-3-cyclopentyl-2-((*N*-hydroxyformamido)methyl)propanoyl)hydrazinyl)-5-fluoro-2-methylpyrimidin-4-yl)-2-<sup>14</sup>C]octahydro-1*H*-pyrazino[2,1-*c*][1,4]oxazin-5-ium

FIG 1 Structural formula of GSK1322322 (with full IUPAC name) and position of the <sup>14</sup>C in the labeled compound.

study were (i) to determine the *in vitro* activity of GSK1322322 using a pharmacodynamic model of intracellular infection in human THP-1 monocytes and various susceptible and resistant strains of *S. aureus* and (ii) to examine its cellular pharmacokinetics (influx, accumulation, efflux, and subcellular localization) in human THP-1 monocytes and murine J774 macrophages. In brief, GSK1322322 proved capable of reducing about 70% to 90% of the intracellular inoculum (0.5 to 1 log<sub>10</sub> CFU decrease), whatever the resistance phenotype of the strain toward other anti-staphylococcal agents. It showed an intracellular disposition close to that of fluoroquinolones (18, 19), with an apparent ability to act on its intracellular target despite its relatively low cellular accumulation levels and absence of stable association with phagolysosomes, where *S. aureus* sojourns and thrives in phagocytic cells (20, 21). This study therefore explored the potential of PDF inhibitors for the treatment of infections caused by *S. aureus* strains resistant to commonly used antibiotics and involving intracellular reservoirs. In a broader and normative context, this report further demonstrates that the intracellular activity of antibiotics cannot be simply deduced from their level of accumulation and subcellular disposition and that part of the intracellular inoculum of *S. aureus* is refractive to the activity of most antibiotics.

(This work was presented in part at the 54th Interscience Conference on Antimicrobial Agents and Chemotherapy [ICAAC], Washington, DC, 5 to 9 September 2014 [22], and at the 24th European Congress of Clinical Microbiology and Infectious Diseases [ECCMID], Barcelona, Spain, 10 to 13 May 2014 [23].)

## MATERIALS AND METHODS

**Antibiotics and main products.** GSK1322322 (potency, 100%) and [<sup>14</sup>C]GSK1322322 (specific activity, 59.9 mCi/mmol; labeled on position 2 of the fluoropyrimidine group [see Fig. 1]; radiochemical purity, 99.5%) were obtained from GlaxoSmithKline plc (Collegeville, PA). The product was first dissolved in dimethyl sulfoxide at a concentration of 50 mg/liter and was thereafter further diluted in water to the desired concentration. The radiolabeled compound was added in a tracing amount to stock solutions of unlabeled GSK1322322 in order to obtain appropriate signals under our experimental conditions. Azithromycin and clarithromycin (potency, 100%) were obtained from SMB-Galephar (Marche-en-Famenne, Belgium); moxifloxacin HCl (potency, 90.9%) from Bayer AG (Wuppertal, Germany); oxacillin monohydrate and clindamycin (potencies, 90% and 91.2%, respectively) from Sigma-Aldrich (St. Louis, MO); and fusidic acid (potency, 100%) from Cemptra Pharmaceuticals (Chapel Hill, NC). The other antibiotics were obtained as the corresponding branded products registered for human parenteral use in Belgium and

complying with the provisions of the European Pharmacopoeia (vancomycin as Vancomycine Mylan [Mylan Inc., Canonsburg, PA], linezolid as Zyvoxid [Pfizer Inc., New York, NY], daptomycin as Cubicin [Novartis, Horsham, United Kingdom], tigecycline as Tygacil [Wyeth Pharmaceuticals; presently, Pfizer Inc.], and gentamicin as gentamicin-80-mg-Rotexmedica [Rotexmedica GmbH, Trittau, Germany]). Gemfibrozil and verapamil were obtained from Sigma-Aldrich (St. Louis, MO), human serum was obtained from Biowest SAS (Nuaillé, France), and cell culture media and sera were obtained from Gibco/Life Technologies Corporation (Paisley, United Kingdom). Unless stated otherwise, all other products were obtained from Sigma-Aldrich or Merck KGaA (Darmstadt, Germany).

**Cell lines.** Experiments were performed with (i) human THP-1 cells (a myelomonocytic cell line; 24) purchased as clone ATCC TIB-202 from the American Tissue Culture Collection, Manassas, VA, and (ii) murine J774 macrophages (derived from a reticulosarcoma; 25) obtained from Sandoz Forschung Laboratories, Vienna, Austria. Both cell lines were maintained in our laboratory as previously described (26, 27).

**Bacterial strains and susceptibility testing.** The laboratory and clinical strains used in the present study are listed in Table 1 with information on their origins and their resistance phenotypes. MICs were determined by microdilution in cation-adjusted Mueller-Hinton broth (CA-MHB; Becton, Dickinson and Company, Franklin Lakes, NJ) following the recommendations of the Clinical and Laboratory Standards Institute (CLSI) (32) with addition of 50 mg/liter Ca<sup>2+</sup> (final cation concentration) for daptomycin.

**Assessment of viability of THP-1 monocytes.** The viability of THP-1 monocytes in the presence of increasing concentrations of GSK1322322 was evaluated by measuring the release of the cytosolic enzyme lactate dehydrogenase (LDH) in the culture medium after 24 h of incubation using a Cytotoxicity Detection Kit<sup>PLUS</sup> [LDH] (Roche Diagnostics GmbH, Mannheim, Germany). The release of LDH was expressed as the percentage of activity detected in the media compared to the total enzymatic activity in the culture.

**Determination of the extracellular and intracellular activities of antibiotics.** For extracellular activity, experiments were performed in CA-MHB with an initial inoculum of 10<sup>6</sup> CFU/ml and results expressed as the change in CFU/ml from the initial inoculum as measured by colony counting. Bactericidal activity was defined as a reduction of 99.9% (3 log<sub>10</sub> CFU/ml decrease) of the total counts. For intracellular activity, cell infection was performed as described previously (21). The changes in the number of CFU from the postphagocytosis inoculum were taken as the response to the antibiotics and plotted as a function of their extracellular concentrations (both in log<sub>10</sub> units) (21, 33). Data were used to fit a sigmoidal Equation function (Hill equation),  $Y = E_{max} + \{E_{min} - E_{max}\} / \{1 + 10^{[\log(EC_{50} - x) \times H]}\}$ , where  $Y$  is the number of CFU (in log<sub>10</sub> units),  $x$  is the log<sub>10</sub> of the extracellular concentration (in milligrams/liter or multiples of MIC),  $E_{max}$  (maximal relative efficacy) is the decrease of CFU compared to the original inoculum for an infinitely large extracellular antibiotic concentration (note that a larger maximal relative activity corresponds to a more negative value of  $E_{max}$ ),  $E_{min}$  (minimal relative efficacy) is the increase in the number of CFU compared with the original inoculum for an infinitely low extracellular antibiotic concentration (this value is positive and corresponds to the increase in CFU in the absence of antibiotic),  $EC_{50}$  is the concentration of antibiotic (in milligrams/liter or in multiples of MIC) at which  $Y$  is halfway between  $E_{min}$  and  $E_{max}$ , and  $H$  is the slope (Hill coefficient; absolute value set by default to 1 [−1 in this case as the function slope is downhill] because of the lack of an indication of any constant cooperative effect). This equation also allowed us to calculate the value of the apparent static concentration ( $C_s$ ) corresponding to the extracellular concentration of drug (expressed in milligrams/liter or in multiples of MIC) causing no apparent change in CFU compared with the initial inoculum using the following rearrangement (see reference 34 and the references cited there and above for detailed descriptions of the protocol and of the interpretation of the corresponding pharmacodynamics

TABLE 1 Strains used in the study, strain origins, and MIC in broth<sup>m</sup>

Strain	Origin	MIC (mg/liter)										
		GSK	AZM	CLR	OXA	CLI	FUS <sup>a</sup>	VAN	DAP <sup>b</sup>	LZD	TGC <sup>c</sup>	MXF
ATCC 29213	— <sup>d</sup>	1	2	0.5	1	0.0625	0.125	1	1–2	2	0.5	0.0625
ATCC 25923	— <sup>e</sup>	1	1	0.25	0.25	0.0625	0.125*–0.25	1	1	2	0.25	0.032–0.125*
SA040	Clinical <sup>f</sup>	0.5*–1	<b>4</b>	1	0.25	ND	ND	0.5–1	1–2	4	0.25–0.5	0.0625
SA040 LZD <sup>R</sup>	Clinical <sup>f</sup>	1	2	0.25	0.25	0.125	0.062*–0.125	1–2	<b>2</b>	<b>16</b>	0.25–0.5	0.125
SA618 bis	Clinical <sup>g</sup>	1	ND	ND	<b>256</b>	ND	ND	<b>4</b>	<b>32</b>	2	0.5	<b>4*–8</b>
NRS119	Clinical <sup>h</sup>	1	<b>4</b>	2	<b>&gt;256</b>	<b>1</b>	0.25	1	<b>2</b>	<b>64</b>	0.5	<b>4</b>
MU50	Clinical <sup>i</sup>	1	<b>&gt;256</b>	<b>&gt;256</b>	<b>&gt;256</b>	<b>&gt;256</b>	0.25	<b>8</b>	<b>8</b>	1	0.5–1	<b>2*–4</b>
VUB09	Clinical <sup>j</sup>	0.5	<b>&gt;256</b>	<b>&gt;256</b>	<b>64</b>	<b>256</b>	0.125	0.5–1	<b>2</b>	2	0.5	<b>4</b>
N6113072	Clinical <sup>k</sup>	0.5	<b>&gt;256</b>	<b>&gt;256</b>	0.25	<b>256</b>	0.25	0.5	<b>2</b>	4	0.25	0.5
SA312	Clinical <sup>l</sup>	1*–2	<b>256</b>	<b>128</b>	<b>64</b>	0.0625	0.125	0.5–1	1–2	2–4	0.5	0.0625

<sup>a</sup> No breakpoint defined by CLSI.

<sup>b</sup> Only the susceptible (“S”) breakpoint ( $\leq 1$  mg/liter) is defined by CLSI.

<sup>c</sup> No breakpoint defined by CLSI (“S” FDA breakpoint,  $\leq 0.5$  mg/liter).

<sup>d</sup> —, laboratory standard (ATCC, Manassas, VA) and EUCAST quality control *Staphylococcus aureus*.

<sup>e</sup> —, laboratory standard (ATCC, Manassas, VA).

<sup>f</sup> Strain from P. Appelbaum, Hershey Medical Center, Hershey, PA (28).

<sup>g</sup> Respiratory tract infection; strain from P. Appelbaum, Hershey Medical Center, Hershey, PA.

<sup>h</sup> See reference 29.

<sup>i</sup> ATCC 700699 (Manassas, VA).

<sup>j</sup> Wound infection; strain from D. Pierard, Universitair Ziekenhuis Brussel, Brussels, Belgium.

<sup>k</sup> See reference 30.

<sup>l</sup> Strain from P. Appelbaum, Hershey Medical Center, Hershey, PA.

<sup>m</sup> Figures in bold italic indicate values greater than the EUCAST resistant (“R”) clinical breakpoint values (31), and those in bold also indicate values greater than or equal to the CLSI “R” clinical breakpoint value (32). Abbreviations: GSK, GSK1322322; AZM, azithromycin; CLR, clarithromycin; OXA, oxacillin; CLI, clindamycin; FUS, fusidic acid; VAN, vancomycin; DAP, daptomycin; LZD, linezolid; TGC, tigecycline; MXF, moxifloxacin; ND, not determined. \*, value used for all calculations.

parameters; see also references 35, 36, 37, and 38 for descriptions of their use in the evaluation of other novel antibiotics):

$$C_S = 10^{([H \times \log EC_{50}] - \log[(E_{\min} - E_{\max})(0 - E_{\max}) - 1]) / H} \quad (1)$$

**Accumulation and release experiments.** Antibiotic accumulation and release were measured using a general protocol developed in our laboratory to study the cellular pharmacokinetics of antibiotics in J774 macrophages and THP-1 monocytes (35, 36, 39–41). In the present experiments, cells were incubated in the presence of GSK1322322 (with a suitable amount of <sup>14</sup>C-labeled drug) in standard culture medium for the lengths of time and at the concentrations adapted for the purpose of each experiment. After removal of the medium, J774 macrophages (adherent) were washed gently three times with ice-cold phosphate-buffered saline (PBS) and THP-1 monocytes (growing in suspension) were subjected to two successive low-speed centrifugations in PBS at 4°C. Cells were then resuspended in distilled water and subjected to sonication (5 min at 100 W in a water bath sonicator [Bransonic ultrasonic cleaner model 3510E-MT; Bransonic, Danbury, CT]) for complete dispersion of visible material and the lysate used for determination of radioactivity (liquid scintillation counting) (Packard Tri-Carb instrument; Perkin-Elmer [Waltham, MA]) and for the protein assay (42). The cell drug content was expressed by reference to the total cell protein content, and the apparent total cellular concentration was then calculated using a conversion factor of 3.08  $\mu$ l of cell volume per mg of cell protein for J774 macrophages (41) and 5  $\mu$ l of cell volume per mg of cell protein for THP-1 monocytes (21).

**Cell fractionation studies.** We followed the general protocol developed in our laboratory for studying the subcellular distribution of antibiotics in cells (19, 26, 40, 43, 44). In the present experiments, uninfected cells were incubated with 1 mg/liter GSK1322322 (with a suitable amount of <sup>14</sup>C-labeled drug) for 30 min, washed, and collected in ice-cold 0.25 M sucrose–3 mM Na EDTA–3 mM imidazole (pH 7.4) (sucrose-EDTA-imidazole), whereas infected cells were exposed to bacteria for phagocytosis as described above, washed, returned to fresh medium for 2 h to allow complete internalization of bacteria, and then incubated for 30 min with GSK1322322 at a total concentration of 0.1 mg/liter (to avoid killing of the bacteria [again with a suitable amount of <sup>14</sup>C-labeled drug]),

washed, and finally collected in sucrose-EDTA-imidazole. Cells were then homogenized in the same medium using a Dounce tissue grinder with control of the cell disruption process by phase-contrast microscopy. Subcellular organelles were separated by differential and isopycnic centrifugation using methods described in detail in the references cited above. In brief, for differential centrifugation, homogenates were separated into 3 successive fractions, namely, fractions N (nuclei and unbroken cells), ML (large granules), and P (small granules and membranes; for some experiments, the ML and P [MLP] fractions were obtained together), and a final S supernate (cytosol) by centrifugation at 1,600, 25,000, and 40,000 rpm for 10 min, 6 min 42 s, and 30 min, respectively, in a Ti50 rotor operated in a Beckman Optima LE-80K ultracentrifuge (Beckman Coulter Life Sciences, Indianapolis, IN). For isopycnic centrifugation, the cell homogenate was first made free of nuclei and unbroken cells by centrifugation at 1,600 rpm for 10 min, and the resulting cytoplasmic extract was deposited on a linear sucrose gradient with densities spanning 1.10 to 1.24 and was left resting on a cushion of sucrose of 1.34 density. After centrifugation at 39,000 rpm for 3 h in a SWTi50 swing-out rotor (Beckman), the gradient was collected into 12 discrete fractions whose densities were measured by refractometry (ABBE-3L refractometer; Bausch and Lomb, Rochester, NY). All fractions were assayed for protein content and activity of marker enzymes (as described in the references cited above) and, if infected, in viable bacteria (for CFU counting).

**Curve fitting and statistical analyses.** Curve fitting and statistical analyses were performed with GraphPad Prism versions 4.03 and 6.05 (GraphPad Software Inc., San Diego, CA), GraphPad InStat v3.10 (GraphPad Software), and JMP Pro version 10.02 and 11.1.1 (SAS Institute Inc., Cary, NC).

## RESULTS

**Susceptibility of *S. aureus* strains to GSK1322322 and comparator antibiotics.** The aim of the study was to establish whether GSK1322322 showed measurable activity against intracellular forms of *S. aureus* that was unaffected by any mechanism(s) of resistance to currently used antistaphylococcal antibiotics. A

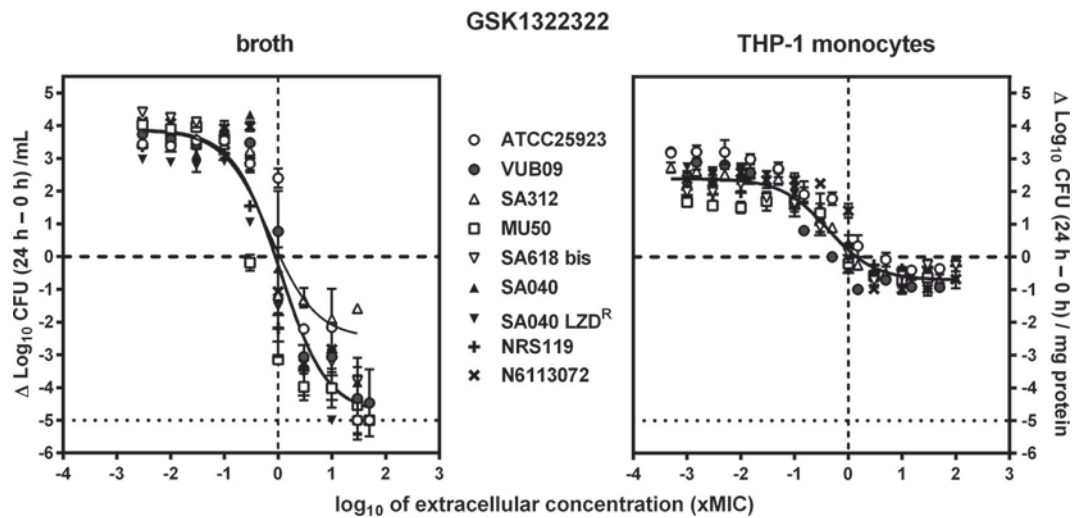


**FIG 2** Concentration-dependent activities of GSK1322322 against extracellular (MHB; pH 7.4 [left panel]) and intracellular (THP-1 monocytes [right panel]) forms of *S. aureus* strains with different resistance phenotypes (see Table 1 for individual MICs and patterns of resistance to the antistaphylococcal agents tested). For these experiments, broths or infected cells were incubated for 24 h in the presence of increasing concentrations of antibiotic (total drug; abscissa [in multiples of MIC in broth]). The ordinates show the change in the number of CFU ( $\log_{10}$ ) per milliliter of medium (broth) or per milligram of cell protein (THP-1). The horizontal dashed line shows a static effect (no apparent change from the initial, postphagocytosis inoculum) and the vertical dashed line the MIC. All values are means  $\pm$  standard errors of the means (SEM) ( $n = 2$  or 3 experiments, with each performed in triplicate; where SEM bars are not visible, they are smaller than the symbols). The lowest limit of detection (horizontal dotted line) corresponds to a CFU decrease of 5  $\log_{10}$  units compared to the original inoculum. Data were used to fit sigmoidal functions (slope factor =  $-1$ ) using all data points for extracellular activities (left) or intracellular activities (thick lines), except for strain SA312 for extracellular bacteria, for which an individual fit (thin line) was calculated, as it was the only strain for which the  $E_{\max}$  value ( $-2.49$  CFU decrease) suggested a nonbactericidal effect. See Table 2 for numeric data of regression parameters, pertinent pharmacodynamic descriptors, and statistical analyses for intracellular activities.

panel of representative strains was therefore assembled from laboratory and clinical isolates with (i) demonstrated susceptibility to the comparator antibiotics in our model (fully susceptible strains) and (ii) resistance of clinical significance to one or several of the comparators (resistant strains). Table 1 shows the strains used and the MICs of GSK1322322 and of the comparator antibiotics for each of the strains. GSK1322322 showed an MIC that was consistently low (0.5 to 1 mg/liter) for all strains, disregarding their resistance patterns to other antibiotics, except for strain SA312 (a methicillin-resistant *S. aureus* [MRSA] strain resistant also to macrolides but not to clindamycin), for which the MIC was 1 dilution higher (1 to 2 mg/liter). Of particular interest was the observation that GSK1322322 remained fully active against strains resistant to vancomycin, daptomycin, or linezolid.

**Cellular viability.** As a preliminary to experiments implying exposure of eukaryotic cells to GSK1322322, we examined the cellular viability of THP-1 cells incubated with concentrations spanning 0.4 to 100 mg/liter by measuring the release of the cytosolic enzyme lactate dehydrogenase in the culture medium. This release remained similar to control values and lower than 8% over the whole range of concentrations investigated (data not shown), which was therefore the level considered for the performance of further experiments.

**Pharmacological descriptors of the extracellular and intracellular activities of GSK1322322 against strains susceptible or resistant to comparators.** In this first series of experiments, 24-h concentration responses were examined for GSK1322322 against all strains in broth (extracellular activity) as well as after phagocytosis by THP-1 monocytes (intracellular activity). In all cases, GSK1322322 activity developed in a concentration-dependent manner, with a single sigmoid function being satisfactorily fitted

to the data for each strain, in accordance with the pharmacological model previously described for other antibiotics against the fully methicillin-susceptible *S. aureus* (MSSA) ATCC 25923 strain (21) and strains with different resistance phenotypes (see typical examples in references 35, 36, and 37). Interestingly enough, when drug concentrations were expressed in multiples of the corresponding MIC, a single function could be fitted to the whole set of data, in broth (except for strain SA312) or intracellularly, demonstrating similar profiles of activity against all strains, as previously described for other antibiotics (33, 37, 38). Thus, in broth (Fig. 2, left panel), the  $E_{\min}$  values were similar for all strains (approximately  $+4 \log_{10}$  CFU over 24 h), a bacteriostatic effect was obtained at a concentration close to the MIC, and the  $E_{\max}$  value reached about  $-4.8 \log_{10}$  CFU (close to the limit of detection) for all strains except SA312, for which an individual fit showed an  $E_{\max}$  of only  $-2.49 \log_{10}$  CFU (repeating the experiment did not significantly change this  $E_{\max}$  value). After phagocytosis (Fig. 2, right panel), intracellular growth spanning CFU increases between 1.75 and 3.11  $\log_{10}$  over 24 h was observed with a ranking of (from largest to smallest value) ATCC 25923 > VUB09 > SA040 LZD<sup>R</sup> > SA312 > N6113072 > SA040 > SA618bis > NRS119 > MU50 (see Table 2 for the corresponding values). For all these strains, GSK1322322 was able to prevent intracellular growth at an extracellular concentration close to its MIC and reduced the extracellular inoculum by 0.5 to 1  $\log_{10}$  CFU compared to the postphagocytosis value at high extracellular concentrations ( $E_{\max}$ ).

We next compared the intracellular activity of GSK1322322 with that of other antibiotics against the fully susceptible laboratory strain ATCC 25923, and the results are presented in Fig. 3A (see also numeric data in Table 2). All antibiotics showed a maximal relative activity ( $E_{\max}$ ) similar to that of GSK1322322 ( $\sim 0.5$

TABLE 2 Pharmacological descriptors, goodness of fit, and statistical analysis of the dose-response studies of the antibiotics against all strains tested in THP-1 monocytes (24 h of incubation)<sup>a</sup>

Antibiotic and strain	$E_{\min}^b$	$E_{\max}^c$	$C_s^d$		$R^2$
			Total concn as a multiple of the MIC (CI)	Concn (mg/liter) (CI)	
<b>GSK1322322</b>					
ATCC 25923	3.11 (2.95 to 3.28) A	-0.45 (-0.66 to -0.23) A	7.19 (6.15 to 6.90) A	7.19 (6.15 to 6.90)	0.97
SA040	2.52 (2.36 to 2.68) C, D	-0.78 (-0.96 to -0.60) A	2.05 (1.62 to 2.65) B	1.02 (0.81 to 1.33)	0.97
SA040 LZD <sup>R</sup>	2.76 (2.58 to 2.93) A, B, C	-0.79 (-0.99 to -0.59) A	0.91 (0.71 to 1.14) B	0.91 (0.71 to 1.14)	0.97
SA618 bis	2.14 (1.94 to 2.34) D, E	-0.51 (-0.69 to -0.34) A	1.31 (0.59 to 2.44) B	1.31 (0.59 to 2.44)	0.95
NRS119	1.98 (1.83 to 2.13) E	-0.42 (-0.56 to -0.28) A	1.42 (1.36 to 1.49) B	1.42 (1.36 to 1.49)	0.96
MU50	1.75 (1.55 to 1.94) E	-0.93 (-1.25 to -0.62) B	1.33 (1.02 to 1.67) B	1.33 (1.02 to 1.67)	0.92
VUB09	3.04 (2.83 to 3.26) A, B	-1.02 (-1.22 to -0.83) B	0.96 (0.89 to 1.03) B	0.48 (0.45 to 0.51)	0.97
N6113072	2.54 (2.30 to 2.77) C, D	-1.18 (-1.53 to -0.84) B	2.68 (2.60 to 2.76) B	1.34 (1.30 to 1.38)	0.93
SA312	2.67 (2.56 to 2.79) B, C	-0.77 (-0.93 to -0.62) A	3.11 (2.65 to 3.64) B	3.11 (2.65 to 3.64)	0.98
<b>Azithromycin</b>					
ATCC 25923	3.31 (3.05 to 3.56) A	-0.56 (-0.97 to -0.15) ns	9.91 (9.11 to 10.8) A; ns	9.91 (9.11 to 10.8) ns	0.95
SA040	2.82 (2.51 to 3.13) A, B, C	-1.12 (-1.36 to -0.88) ns	0.29 (0.22 to 0.37) B; *>	1.17 (0.90 to 1.47) ns	0.96
NRS119	2.22 (1.95 to 2.48) C	-0.34 (-0.53 to -0.15) *<	0.59 (0.40 to 0.84) B; ns	2.35 (1.60 to 3.35) ns	0.95
MU50	No convergence	1.92 (1.84 to 1.99) *<	No convergence	No convergence	0.11
VUB09	3.05 (2.61 to 3.49) A, B	2.89 (2.81 to 2.96) *<	No convergence	No convergence	0.12
N6113072	2.56 (2.47 to 2.64) B, C	No convergence	No convergence	No convergence	0.03
SA312	2.48 (2.31 to 2.65) C	-1.53 (-2.18 to -0.87) ns	0.83 (0.63 to 1.09) B; *>	213 (162 to 280) *<	0.96
<b>Clarithromycin</b>					
ATCC 25923	3.35 (3.06 to 3.65) A	-0.38 (-0.73 to -0.04) ns	4.90 (4.42 to 5.37) A; ns	1.23 (1.10 to 1.34) *>	0.95
MU50	2.05 (1.93 to 2.17) D	1.98 (1.89 to 2.07) *<	No convergence	No convergence	0.08
VUB09	3.15 (2.53 to 3.76) B	2.80 (2.74 to 2.85) *<	No convergence	No convergence	0.42
N6113072	2.66 (2.56 to 2.77) C	2.56 (2.48 to 2.64) *<	No convergence	No convergence	0.17
SA312	2.73 (2.48 to 2.98) C	-0.82 (-1.39 to -0.24) ns	1.34 (0.91 to 1.86) B; *>	172 (116 to 238) *<	0.93
<b>Oxacillin</b>					
ATCC 25923	3.35 (3.17 to 3.53) A	-0.91 (-1.07 to -0.75) ns	0.52 (0.48 to 0.57) A; *>	0.13 (0.12 to 0.14) *>	0.99
SA618 bis	2.07 (1.92 to 2.22) B	-1.56 (-4.07 to 0.95) *>	1.15 (0.83 to 1.65) A; ns	293 (214 to 422) *<	0.91
NRS119	2.09 (1.90 to 2.28) B	-1.39 (-2.72 to -0.053) ns	No convergence	418 (262 to 620) *<	0.89
MU50	2.03 (1.82 to 2.25) B	-1.34 (-2.67 to -0.008) ns	No convergence	1,224 (687 to 1,980) *<	0.86
VUB09	3.06 (2.73 to 3.40) A	-0.76 (-0.97 to -0.54) ns	0.01 (0.01 to 0.02) B; *>	0.94 (0.80 to 1.09) *<	0.97
SA312	2.95 (2.73 to 3.17) A	-0.91 (-1.13 to -0.69) ns	0.10 (0.10 to 0.11) B; *>	6.36 (6.10 to 6.75) *<	0.98
<b>Clindamycin</b>					
ATCC 25923	3.55 (3.41 to 3.69) A	-0.66 (-0.91 to -0.41) ns	13.1 (11.9 to 14.4) A; *<	0.82 (0.74 to 0.90) *>	0.98
NRS119	2.09 (1.90 to 2.28) E	-0.48 (-0.67 to -0.29) ns	3.48 (2.72 to 4.35) B; *<	3.48 (2.72 to 4.35) *<	0.97
MU50	2.13 (2.01 to 2.26) D	2.03 (1.92 to 2.14) *<	No convergence	No convergence	0.10
VUB09	2.79 (2.70 to 2.88) B	2.80 (2.68 to 2.92) *<	No convergence	No convergence	0.00
N6113072	2.32 (2.24 to 2.39) C	2.15 (2.08 to 2.22) *<	No convergence	No convergence	0.43
<b>Fusidic acid</b>					
ATCC 25923	3.62 (3.31 to 3.93)	-1.19 (-1.94 to -0.44) *>	19.6 (15.6 to 23.9) *<	2.46 (1.95 to 2.99) *>	0.93
<b>Vancomycin</b>					
ATCC 25923	3.29 (3.02 to 3.56) A	-0.96 (-1.46 to -0.46) ns	9.18 (7.59 to 9.84) A; ns	9.18 (7.59 to 9.84) ns	0.95
SA618 bis	2.09 (1.80 to 2.38) B	-0.80 (-1.16 to -0.45) ns	1.56 (1.07 to 2.12) B; ns	6.23 (4.28 to 8.46) *<	0.93
MU50	2.13 (1.89 to 2.37) B	-0.57 (-0.80 to -0.34) ns	1.29 (0.96 to 1.83) B; ns	10.3 (7.71 to 14.6) *<	0.95
<b>Daptomycin</b>					
ATCC 25923	3.81 (3.44 to 4.18) A	-0.80 (-1.176 to -0.41) ns	2.04 (1.05 to 3.67) A; *>	2.04 (1.05 to 3.67) *>	0.96
SA040 LZD <sup>R</sup>	3.25 (2.91 to 3.59) B	-0.35 (-0.62 to -0.08) *<	1.18 (0.95 to 1.94) A; ns	2.36 (1.88 to 2.91) *<	0.95
SA618 bis	1.99 (1.70 to 2.29) E	-0.76 (-1.08 to -0.42) ns	0.49 (0.47 to 0.52) A; ns	15.7 (14.9 to 16.5) *<	0.93
NRS119	2.44 (2.20 to 2.68) C, D	-0.44 (-0.67 to -0.20) ns	1.92 (1.80 to 2.05) A; ns	3.85 (3.61 to 4.10) *<	0.95
MU50	2.07 (1.87 to 2.27) D, E	-0.70 (-0.93 to -0.47) ns	2.04 (1.90 to 2.23) A; ns	16.3 (15.2 to 18.0) *<	0.96
VUB09	2.80 (2.49 to 3.12) C	-0.74 (-1.14 to -0.35) ns	2.47 (1.73 to 3.39) A; *<	4.95 (3.46 to 6.78) *<	0.94
N6113072	2.70 (2.34 to 3.07) C	-1.00 (-1.44 to -0.56) ns	1.75 (1.42 to 2.11) A; *>	3.51 (2.84 to 4.22) *<	0.92

(Continued on following page)

TABLE 2 (Continued)

Antibiotic and strain	$E_{\min}^b$	$E_{\max}^c$	$C_s^d$		$R^2$
			Total concn as a multiple of the MIC (CI)	Concn (mg/liter) (CI)	
<b>Linezolid</b>					
ATCC 25923	3.29 (3.10 to 3.49) A	-0.78 (-0.99 to -0.57) ns	2.30 (2.20 to 2.40) A; *>	4.60 (4.40 to 4.79) *>	0.98
SA040	2.47 (2.22 to 2.72) C	-1.27 (-1.54 to -0.99) ns	1.12 (0.98 to 1.27) A; ns	4.47 (3.92 to 5.08) *<	0.97
SA040 LZD <sup>R</sup>	3.14 (2.87 to 3.40) A, B	-0.25 (-0.51 to 0.01) *<	3.66 (1.74 to 6.79) A; ns	58.6 (27.8 to 108) *<	0.96
NRS119	2.69 (2.45 to 2.93) B, C	-1.31 (-1.82 to -0.81) *>	1.08 (0.74 to 1.50) A; ns	69.3 (47.1 to 96) *<	0.95
<b>Tigecycline</b>					
ATCC 25923	3.72 (3.37 to 4.07)	-1.03 (-1.45 to -0.61) *>	2.88 (1.84 to 4.05) *>	0.72 (0.46 to 1.01) *>	0.96
<b>Moxifloxacin</b>					
ATCC 25923	3.29 (2.98 to 3.61) A	-1.71 (-2.12 to -1.31) *>	1.11 (0.99 to 1.24) A; *>	0.14 (0.12 to 0.16) *>	0.97
SA618 bis	2.49 (2.20 to 2.79) C	-1.23 (-1.61 to -0.84) *>	1.70 (1.13 to 2.42) A, B; ns	6.81 (4.51 to 9.68) *<	0.94
NRS119	2.23 (1.91 to 2.54) C, D	-2.11 (-2.54 to -1.68) *>	1.10 (0.78 to 1.47) A; ns	4.42 (3.12 to 5.88) *<	0.95
MU50	2.13 (1.82 to 2.43) D	-2.42 (-2.91 to -1.93) *>	1.91 (1.87 to 1.94) A, B; ns	3.82 (3.75 to 3.88) *<	0.95
VUB09	2.93 (2.64 to 3.22) B	-1.16 (-1.40 to -0.92) ns	0.44 (0.28 to 0.65) C; *>	1.78 (1.12 to 2.58) *<	0.97

<sup>a</sup> Data are from Fig. 2 and 3 and from additional experiments (not illustrated). In statistical analyses, next to the data corresponding to the  $E_{\min}$  and  $E_{\max}$  responses of different strains to the same antibiotic, different uppercase letters indicate that values are significantly different from each other by an analysis of variance (ANOVA) in which all values are compared by the Tukey-Kramer multiple-comparison  $t$  test ( $P < 0.05$ ). Next to the  $C_s$  values, different uppercase letters indicate that the responses are significantly different from each other by an analysis of variance in which first all values and then two individual values are compared using an unpaired (two-tailed)  $t$  test. Additionally, the response of the same strain to each antibiotic and its response to GSK1322322 are compared in an unpaired two-tailed  $t$  test (\*, significant at  $P > 0.05$ ); the sign indicates whether the antibiotic is less (<) or more (>) efficacious ( $E_{\max}$ ) or less or more potent ( $C_s$ ) than GSK1322322 (note that a larger efficacy value corresponds to a more negative  $E_{\max}$  value and a larger potency value to a lower  $C_s$  value). "ns" next to values indicates that the results of the comparison were not statistically significant.

<sup>b</sup> CFU increase (in  $\log_{10}$  units, with confidence interval) at 24 h from the corresponding initial inoculum as extrapolated from the Hill equation of the concentration-effect response (slope factor = -1) for an infinitely low antibiotic concentration.

<sup>c</sup> CFU decrease (in  $\log_{10}$  units, with confidence interval) at 24 h from the corresponding initial inoculum as extrapolated from the Hill equation of the concentration-effect response (slope factor = -1) for an infinitely large antibiotic concentration.

<sup>d</sup> Data represent extracellular total antibiotic concentrations (in multiples of the MIC or in milligrams per liter, with confidence intervals [CI]) resulting in no apparent bacterial growth (static effect) as determined from the Hill equation.

to 1  $\log_{10}$  CFU decrease), except moxifloxacin, for which the  $E_{\max}$  reached a decrease of  $\sim 1.75 \log_{10}$  CFU. When data were plotted against weight concentrations, relative potencies ( $C_s$ ) spanned from 0.13 for oxacillin to 9.18 mg/liter for vancomycin. When data were plotted against multiples of MIC (equipotent concentrations), all antibiotics showed rather similar dose-concentration effects over a relatively narrow range, with  $C_s$  values ranging from 0.52-fold the MIC for oxacillin to 19.6-fold the MIC for fusidic acid, which is in line with our previous observations (45, 46).

In the next series of experiments, we examined the intracellular activity of GSK1322322 against strains resistant to the main anti-MRSA comparators. Results are shown graphically in Fig. 3B, where the data are limited, for sake of clarity, to the results from strains resistant to the comparators and to the antibiotics affected by resistance mechanisms (see Table 2 for numerical data, including those from additional susceptible and resistant strains tested with each pertinent antibiotic). In all cases, GSK1322322 was as effective against the resistant strains as against the susceptible ATCC 25923 strain whereas the comparators did not cause any change in CFU over the whole range of concentrations investigated when the corresponding MIC was  $>256$  mg/liter (see, e.g., macrolides against VUB09) or showed a concentration-effect response that was markedly shifted to higher values but with a relative potency ( $C_s$ ) remaining in the range of their respective MICs (for the strains for which the drug MICs were  $<256$  mg/liter). Oxacillin exhibited divergent behavior, with  $C_s$  values much lower than its MIC, due to the enhancing effect of intraphagolysosomal pH on the activity of this antibiotic as observed previously (47). This effect, however, was not observed for all the MRSA strains

tested here, some of them remaining fully resistant to oxacillin intracellularly. Note also that for several resistant strains, no convergence could be obtained by nonlinear regression for the comparator due to lack of intracellular activity, which prevented us from calculating meaningful pharmacodynamics parameters. Lastly, we used strain NRS119 to confirm that residual bacteria reisolated from THP-1 monocytes at the end of incubation with moxifloxacin showed an unaltered drug MIC, ruling out the selection of a resistant subpopulation.

#### Cellular influx and accumulation and efflux of GSK1322322.

In these experiments, we examined the influx, accumulation level, and efflux of radiolabeled [<sup>14</sup>C]GSK1322322 in uninfected cells exposed to a microbiologically meaningful extracellular concentration of 1 mg/liter. The main experiments were performed with THP-1 monocytes, but J774 macrophages were also used for comparison or for specific experiments. We also tested for an effect of the concentration over a wide range of concentrations and for the influence of temperature on accumulation and efflux. Results are presented in Fig. 4. Accumulation of GSK1322322 in THP-1 monocytes was very rapid, with a plateau reached at an apparent cellular-concentration-to-extracellular-concentration ratio of  $\sim 4$  within 2 min (top left panel). Almost identical images were observed with respect to efflux results (top right panel). Accumulation of GSK1322322 was of the same order of magnitude in THP-1 monocytes and J774 macrophages and was not modified by increasing the concentration of GSK1322322 to 100 mg/liter (lower left panel). It was also markedly impaired when incubation of THP-1 monocytes was carried out at 4°C. Likewise, efflux of GSK1322322 from THP-1 cells loaded at 37°C was totally inhibited.

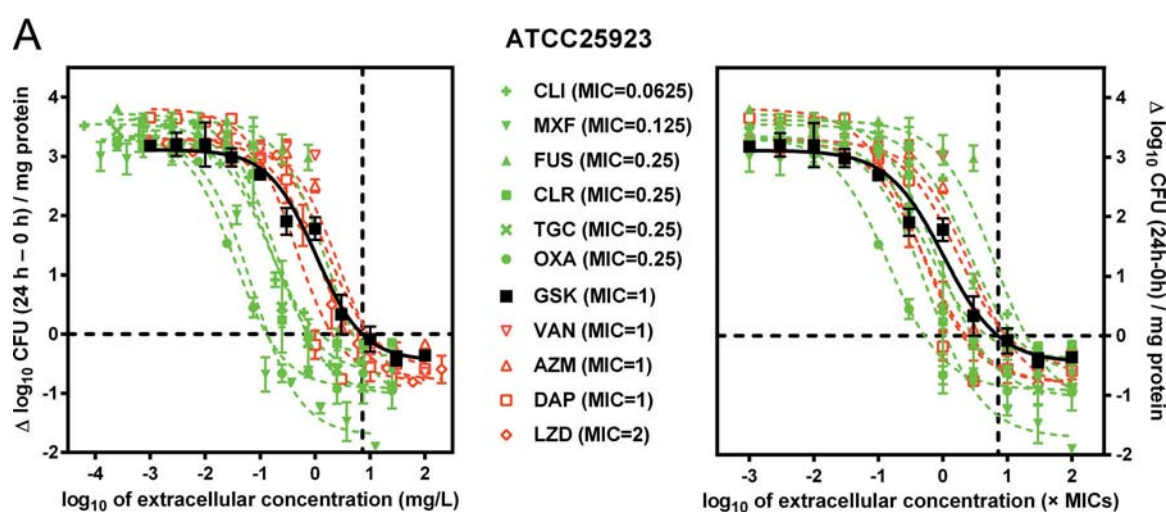


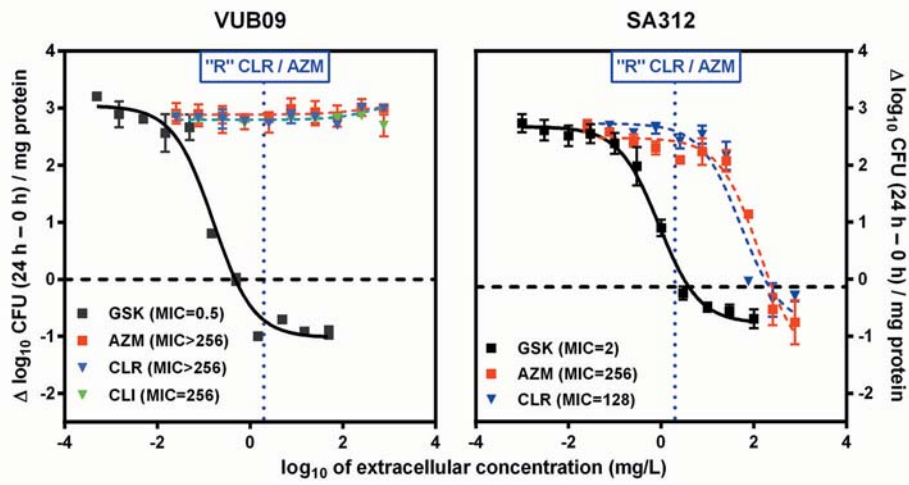
**FIG 3** (A) Concentration-response curves of the intracellular activity of GSK1322322 (GSK) and comparators (CLI, clindamycin; MXF, moxifloxacin; FUS, fusidic acid; CLR, clarithromycin; TGC, tigecycline; OXA, oxacillin; VAN, vancomycin; AZM, azithromycin; DAP, daptomycin; LZD, linezolid) against the (MSSA) ATCC 25923 laboratory strain phagocytized by THP-1 monocytes. The MICs (in milligrams/liter) of the antibiotics against this strain are shown along with the symbols as indicated in the middle of the graph. The ordinates show the changes in the  $\log_{10}$  CFU per milligram of cell protein after 24 h of incubation compared to the postphagocytosis inoculum ( $6.46 \pm 0.12 \log_{10}$  CFU/mg protein [means  $\pm$  standard deviations [SD] of the results from all experiments;  $n = 13$ ]); the horizontal dashed line shows, therefore, a static effect). The abscissa shows the drug concentration expressed as follows: left panel, actual total extracellular concentrations ( $\log_{10}$  milligrams per liter); right panel, actual total extracellular concentrations expressed as  $\log_{10}$  of multiples of the corresponding MIC. For both panels, the vertical dashed line shows the concentration at which GSK1322322 exerts a static effect ( $C_s$ ). Data are means  $\pm$  SEM of data from 3 experiments for GSK1322322 and of data from 2 experiments for the other antibiotics, each performed in triplicate (where SEM bars are not visible, they are smaller than the symbols) and used to fit a (sigmoid) Hill equation with the slope factor set to  $-1$ . Color code: GSK1322322 data and regression lines are shown in black; green data points and regression lines (dotted) represent antibiotics with an MIC lower than that of GSK1322322; red data points and regression lines (dotted) represent antibiotics with an MIC greater than or equal to that of GSK1322322. See Table 2 for numeric data of regression parameters, pertinent pharmacodynamic descriptors, and statistical analyses. (B) Concentration-response curves of the intracellular activity of GSK1322322 (GSK) toward strains with resistance to comparators and phagocytized by THP-1 monocytes. To facilitate the visualization of the results, only data pertaining to GSK1322322 and to the key comparators for each strain are shown, together with their corresponding MICs in broth (see Table 1 for the MICs and Table 2 for numeric data corresponding to the intracellular activity of each antibiotic tested for each strain). Abbreviations: GSK, GSK1322322; AZM, azithromycin; CLR, clarithromycin; CLI, clindamycin; VAN, vancomycin; DAP, daptomycin; LZD, linezolid. The ordinates show the changes in the  $\log_{10}$  CFU per milligram of cell protein after 24 h of incubation compared to the postphagocytosis inoculum ( $6.69 \pm 0.16 \log_{10}$  CFU/mg protein [means  $\pm$  SD of all experiments;  $n = 25$ ]); the horizontal dashed line shows, therefore, a static effect. The abscissa shows the drug concentration expressed as  $\log_{10}$  of the actual total extracellular concentrations in milligrams/liter. For all panels, the vertical blue dotted line shows the concentration corresponding to the EUCAST resistance (“R”) breakpoint (bacteria with an MIC greater than than this value are considered to be clinically resistant). Data represent the means  $\pm$  SEM of the results of 3 independent experiments for GSK1322322 and 2 experiments for the other antibiotics, each performed in triplicate (where SEM bars are not visible, they are smaller than the symbols) and used to fit a Hill equation (sigmoid) with the slope factor set to  $-1$ . Table 2 shows numeric data of regression parameters, pertinent pharmacodynamic descriptors, and statistical analyses.

ited at 4°C (right lower panel). Lastly, we examined the influence of two well-known inhibitors of eukaryotic drug transporters, verapamil and gemfibrozil, using J774 macrophages, for which the role of the corresponding transporters in efflux of the macrolide azithromycin and the fluoroquinolone ciprofloxacin has been clearly demonstrated (39, 41). Using 3 widely differing GSK1322322 concentrations (1, 10, and 100 mg/liter) and concentrations of the inhibitors known to fully inhibit the corresponding transporter, no significant effect was seen, except for verapamil, which caused an increase in GSK1322322 accumulation only at the 10 mg/liter concentration (data not shown).

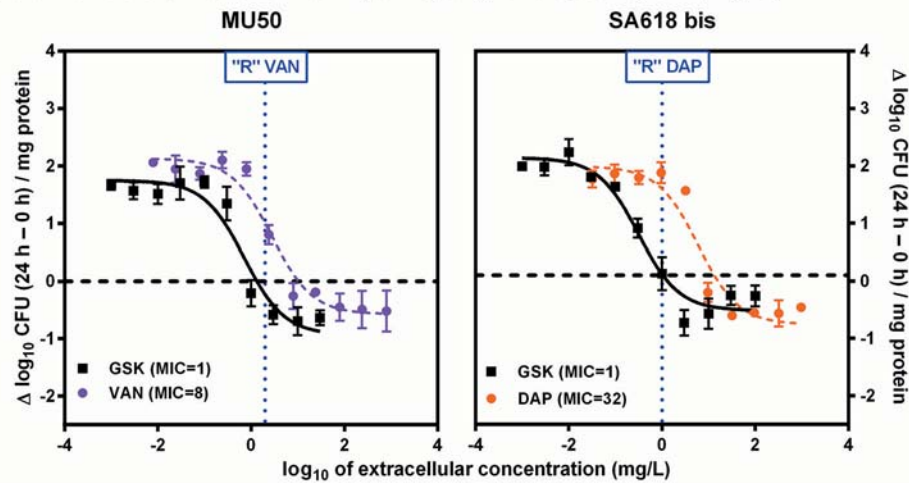
**Subcellular distribution of GSK1322322 in uninfected and infected cells.** In the first experiments of this series, uninfected cells were incubated with GSK1322322 for 30 min (with a suitable amount of  $^{14}\text{C}$ -labeled drug), collected, and homogenized using conditions that largely maintained the integrity of the subcellular organelles. Homogenates (which contained, on a cell protein basis, an amount GSK1322322 similar to what had been observed in the accumulation experiments) were then subjected to differential centrifugation, where organelles are mainly separated on basis of their size, and the distribution of radioactivity was compared to

that of marker enzymes. Figure 5 shows the results of these experiments for THP-1 monocytes (left) and murine J774 macrophages (right). In both cell types,  $^{14}\text{C}$ GSK1322322 was mainly recovered in the final supernatant, with much smaller amounts and no enrichment (on a protein basis) in the other fractions. The distribution of  $^{14}\text{C}$ GSK1322322 was similar to that of lactate dehydrogenase, an enzyme known to be mainly found in the cell cytosol. In contrast, cytochrome *c*-oxidase (marker of mitochondria) and N-acetyl- $\beta$ -hexosaminidase (marker of lysosomes) were found predominantly and enriched in the ML (THP-1 monocytes) or the MLP (J774 macrophages) fractions, with only minimal amounts in the final supernatant. To further discriminate a potential association of a minor proportion of GSK1322322 with lysosomes or mitochondria from its presence in the ML fraction due to contamination by cytosol, an homogenate of J774 macrophages incubated in the presence of  $^{14}\text{C}$ GSK1322322 and made free of nuclei and unbroken cells was deposited on a sucrose gradient and subjected to centrifugation. This method allows separation of lysosomes from mitochondria (on the basis of their buoyant densities), while soluble constituents remain on the top of the gradient. Results illustrated in Fig. 6 show that lysosomes

**B 1. strains resistant to macrolides**



**2. strains resistant to vancomycin (left) or daptomycin (right)**



**3. strains resistant to linezolid**

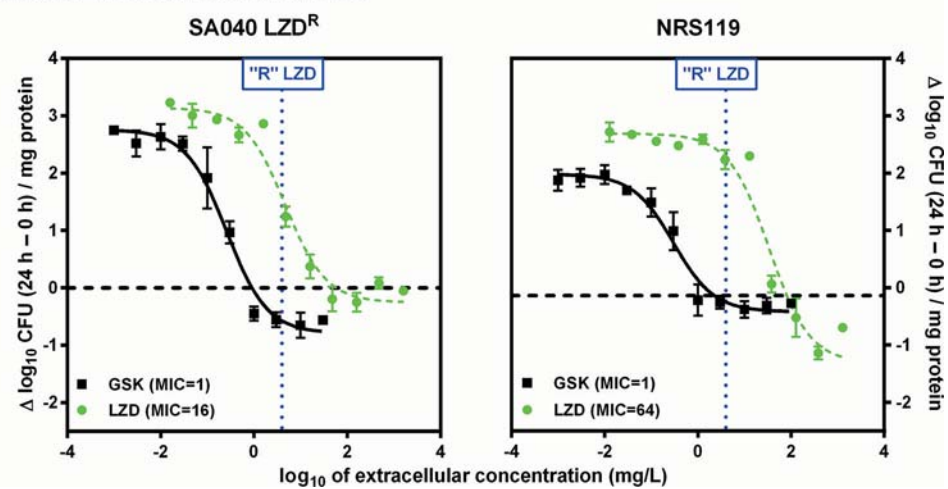
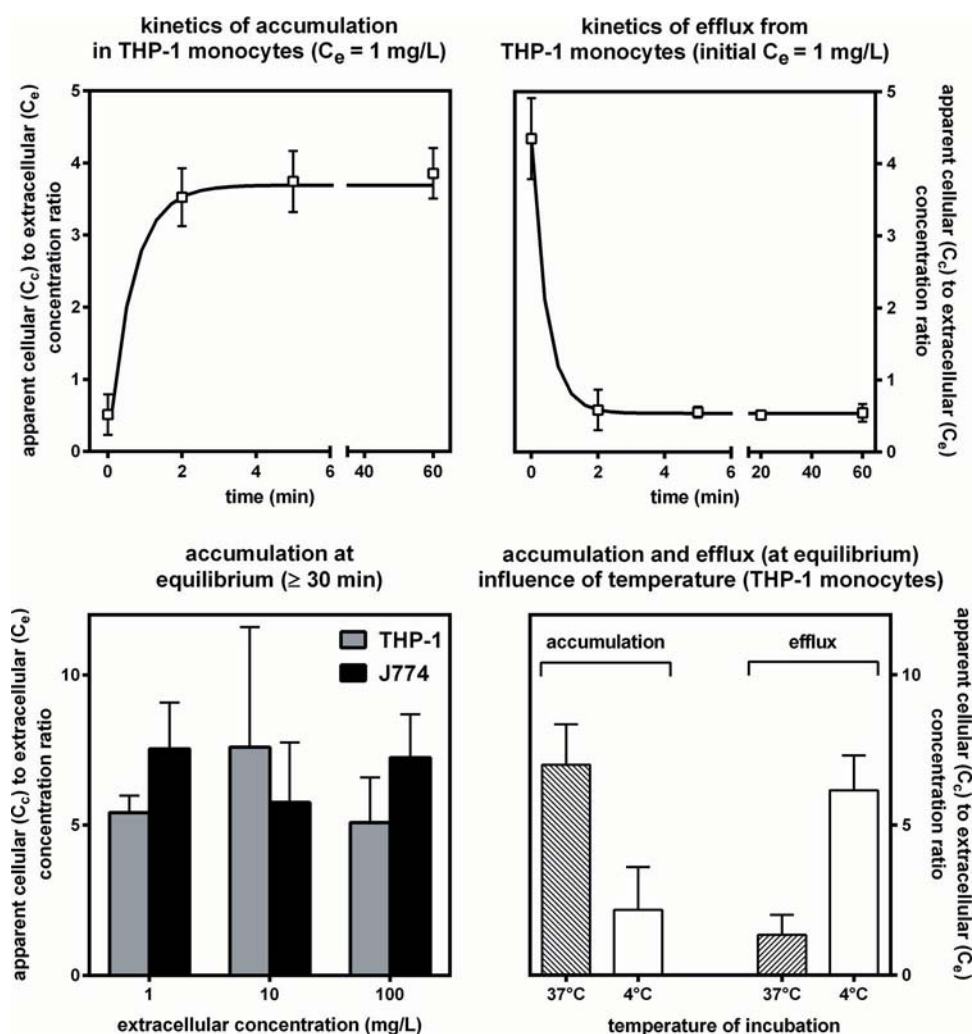


FIG 3 continued



**FIG 4** Kinetics of accumulation and release of GSK1322322 in human THP-1 monocytes and murine J774 macrophages. (Upper graphs) THP-1 monocytes were incubated with [ $^{14}$ C]GSK1322322 at a fixed concentration (1 mg/liter) and cells collected after the times indicated in the abscissa (accumulation; left panel) or incubated for 30 min and then returned to drug-free medium for the times indicated in the abscissa (efflux; right panel). (Lower graphs) Cells were incubated with [ $^{14}$ C]-labeled GSK1322322 for 30 min (THP-1 monocytes) or 1 h (J774 macrophages) at the extracellular concentrations shown in the abscissa (left panel). THP-1 monocytes were incubated for 30 min with 1 mg/liter [ $^{14}$ C]GSK1322322 at the temperatures indicated in the abscissa and collected (accumulation) or incubated for 30 min with 1 mg/liter [ $^{14}$ C]GSK1322322 at 37°C and then returned to drug-free medium for 30 min at the temperatures indicated in the abscissa (efflux) (right panel). For each graph, the ordinate shows the apparent ratio between the cellular and the extracellular concentrations, as determined by the level of radioactivity in cells (based on cell protein assay and assuming a cell volume of 5  $\mu$ l/mg protein for THP-1 monocytes and 3.08  $\mu$ l/mg protein for J774 macrophages) compared to that in the medium. All data are means  $\pm$  SD of the results of 3 independent determinations, with each assay performed in triplicate. Statistical analysis of the influence of concentration on [ $^{14}$ C]GSK1322322 accumulation (lower left panel): none of the differences are statistically significant (one-way analysis of variance [ANOVA] for all data,  $P = 0.53$ ; for THP-1 monocyte data,  $P = 0.45$ ; and for J774 data,  $P = 0.43$ ; unpaired  $t$  test for each of the 2-by-2 comparisons,  $P > 0.14$ ).

and mitochondria were effectively well separated but that [ $^{14}$ C]GSK1322322 and lactate dehydrogenase had essentially remained in a zone corresponding to the position of the sample placed on the gradient and of the very first fractions, with minimal association with the fractions enriched in N-acetyl- $\beta$ -hexosaminidase or cytochrome  $c$ -oxidase (a similar experiment could not be performed with THP-1 monocytes because lysosomes and mitochondria are not well separated on the basis of their buoyant densities in these cells).

In the last series of these experiments, we repeated the differential centrifugation studies using an homogenate of THP-1 monocytes that had been infected with ATCC 25923, reincubated for 2 h, and

then exposed to [ $^{14}$ C]GSK1322322 for 30 min at a concentration corresponding to 1/10 of its MIC to ensure the absence of a notable effect of the antibiotic on the survival of the bacteria. Cells (that had accumulated GSK1322322 at a level corresponding to about 4-fold, as in uninfected cells) were homogenized and subjected to a simplified fractionation procedure to decrease the risks of contamination occurring during the experiment. Results illustrated in Fig. 7 show that both [ $^{14}$ C]GSK1322322 and lactate dehydrogenase were collected in the final supernatant, as in the uninfected cells, whereas bacteria (measured as CFU) were collected only in the MLP fraction, where the bulk of cytochrome  $c$ -oxidase and N-acetyl- $\beta$ -hexosaminidase was also found.

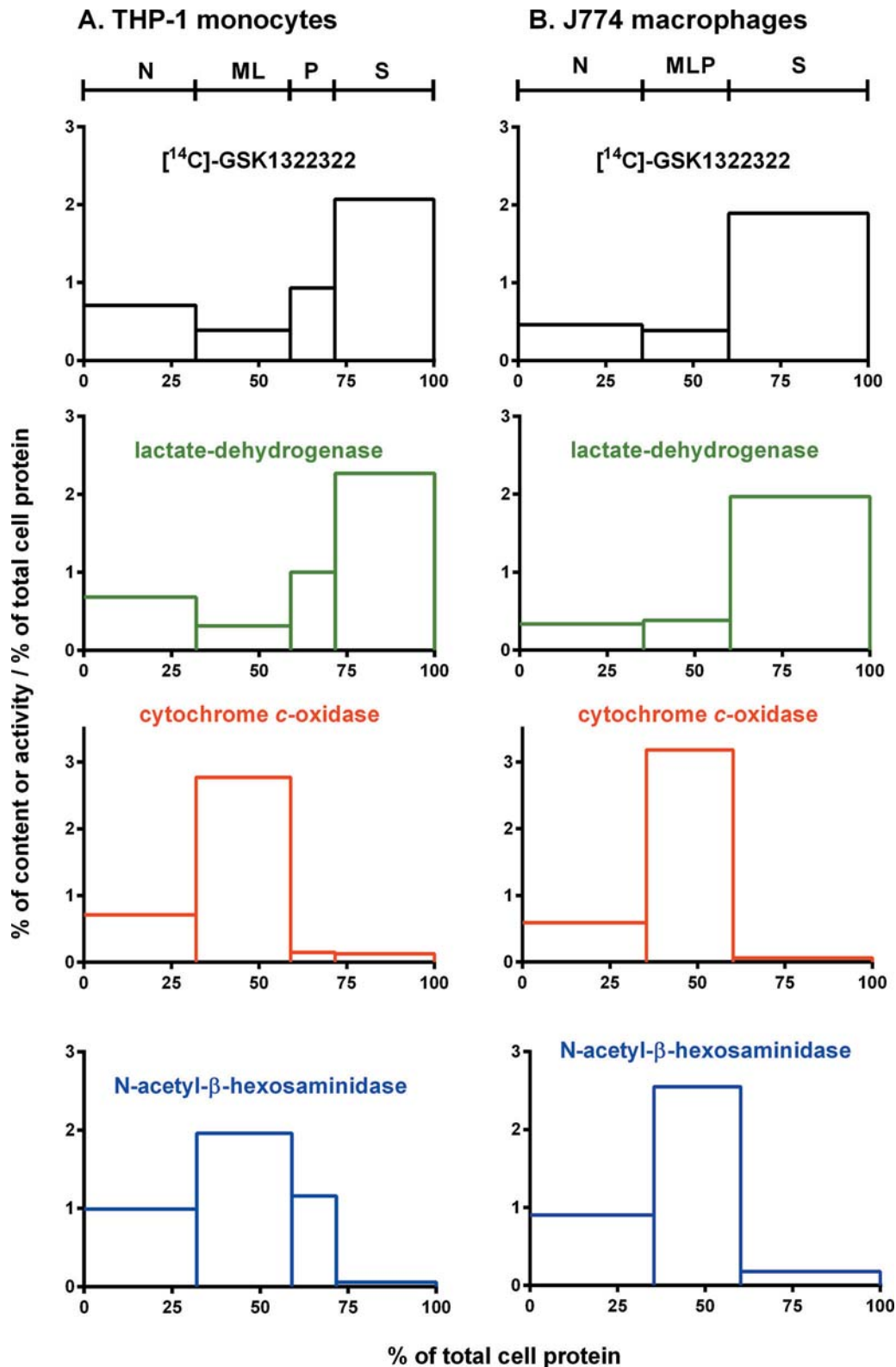


FIG 5 Subcellular distribution of [<sup>14</sup>C]GSK1322322 and of marker enzymes (lactate dehydrogenase, cytosol; cytochrome *c*-oxidase, mitochondria; N-acetyl-β-hexosaminidase, lysosomes) in homogenates of THP-1 monocytes (A) or J774 macrophages (B) incubated with 1 mg/liter [<sup>14</sup>C]GSK1322322 for 30 min prior to collection. The homogenates were separated into 4 (THP-1 monocytes) or 3 (J774 macrophages) fractions (by centrifugation at increasing centrifugal fields) as indicated by letters on the top of the graph (for the main cytological content, N, nuclei and unbroken cells; ML, large granules [mitochondria, lysosomes]; P, small granules [endoplasmic reticulum and Golgi apparatus and plasma membrane fragments]; S, final supernatant). They are represented by blocks ordered in the same sequence over the abscissa, where they span a length proportional to their relative protein content (as a percentage of total cell protein). The height of each block (ordinate) indicates the relative specific content (for [<sup>14</sup>C]GSK1322322) or activity (for marker enzymes), i.e., the percentage recovered in the fraction divided by the percentage of total cell protein of the same fraction. The height of each block therefore indicates the enrichment (if >1) or impoverishment (if <1) of each constituent in the fraction on a protein basis compared to an unfractionated homogenate, while its surface is proportional to the content or activity recovered in the fraction (the total surface of each diagram is given a value of 1). Data are the means of the results of 2 experiments with very similar results.

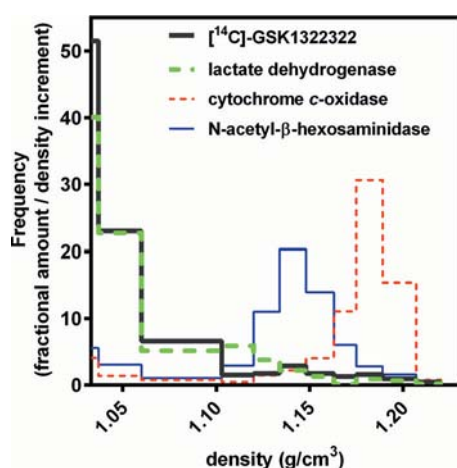


FIG 6 Fractionation of cytoplasmic extracts (homogenates minus the N fraction) of J774 macrophages by density equilibration in a linear sucrose gradient (collected in 12 discrete fractions). Cells were incubated with 1 mg/liter [ $^{14}\text{C}$ ]GSK1322322 for 30 min prior to collection. Results are presented as histograms of density distribution of [ $^{14}\text{C}$ ]GSK1322322 and of the marker enzymes (as described for Fig. 5). The abscissa is the density span of the gradient. The ordinate is the frequency of distribution defined as the fractional amount of activity recovered in each fraction divided by the density interval of that fraction. The surface of each section of the diagrams therefore represents the fraction of each constituent recovered in the corresponding density span and its height the purification achieved on a buoyant-density basis. The total surface of each histogram is 1. Data are the means of the very similar results of 2 experiments.

## DISCUSSION

The present study was, to our knowledge, the first to document the activity of a PDF inhibitor against the intracellular forms of *S. aureus* using a well-established pharmacodynamic model (34) that proved suitable for other clinically used as well as novel antibiotics (21, 33, 35, 36, 38) and predictive of the activity observed in animal models of intracellular infection with *S. aureus* (48, 49).

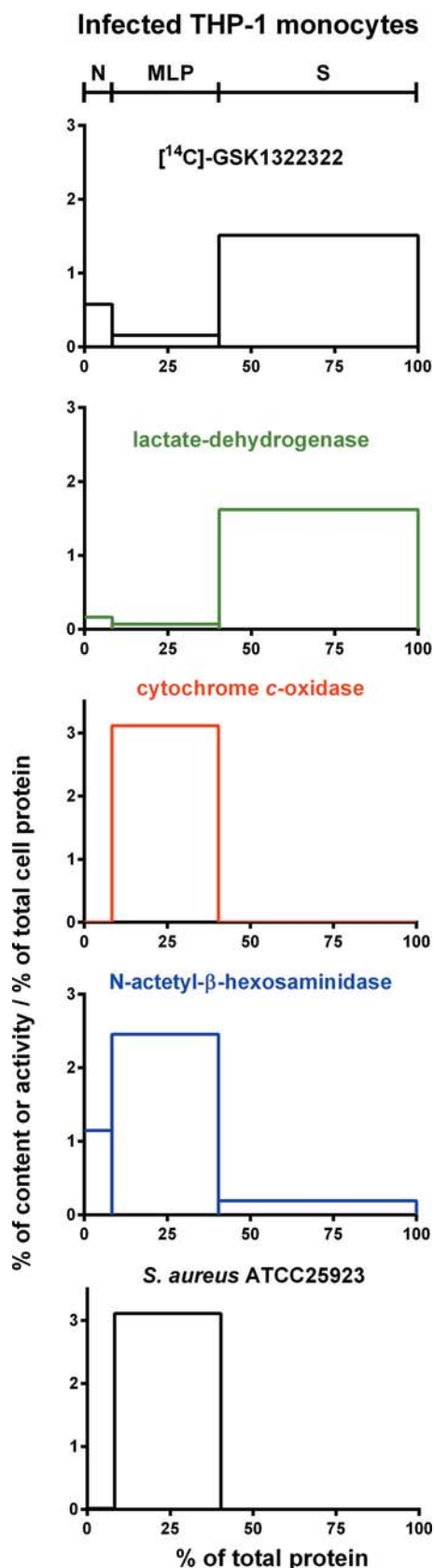
We confirmed that GSK1322322 is a potent antistaphylococcal agent with low and similar MICs against a panel of laboratory and clinical strains of *S. aureus* with resistance to several of the antistaphylococcal agents in current clinical use. Using the pharmacodynamic model, we showed that GSK1322322 is highly bactericidal in broth, reducing the inoculum of  $\sim 4.5 \log_{10}$  CFU within 24 h for most strains, in accordance with previous published data (16), except for strain SA312, where the  $E_{\text{max}}$  value was close to but did not reach the  $3 \log_{10}$  CFU decrease defining a bactericidal effect (32). This is quite similar to what can be obtained with known bactericidal antibiotics such as aminoglycosides or fluoroquinolones (21) or with the recently described anti-MRSA cephalosporin ceftaroline (38) in the same model. This further supports the concept that GSK1322322 has the ability to act on most resistant strains, disregarding their mechanism of resistance to other antibiotics, being directed toward a unique and so far clinically unexploited target. Further experiments, however, will need to examine whether the lower maximal efficacy of GSK1322322 against strain SA312 is unique or is shared with other clinical strains.

Moving now to intracellular bacteria, the pharmacodynamic model shows also that the efficacy of GSK1322322 is considerably reduced in tests against the intracellular forms of *S. aureus*, with  $E_{\text{max}}$  values not exceeding  $-0.5$  to  $-1 \log_{10}$  CFU compared to the

initial postphagocytosis inoculum. In contrast, the relative potency ( $C_s$ ) of GSK1322322 remains essentially similar to the value observed for bacteria in broth. This behavior is not unique to GSK1322322 since it was also observed here for comparators known to be bactericidal in broth such as oxacillin and daptomycin and was clearly documented in previous studies performed with ceftaroline (38) and ceftobiprole (37). It is important that this apparent loss of efficacy cannot be considered to have been due to insufficient penetration or intracellular inactivation, which would have instead affected the relative potency ( $C_s$ ) of the drug (see reference 34 for a review). Affecting only the  $E_{\text{max}}$  value actually indicates that a part of the inoculum had become refractive to the activity of the antibiotics, whatever their extracellular concentration. Thus, in many respects, what we saw here is reminiscent of what was observed for *S. aureus* in an *in vitro* 24-h model of biofilms where the maximal relative efficacy was also considerably reduced (50). This may possibly be related to the development of a so-called persister phenotype (51), well established to take place in biofilms (52). Interestingly enough, the size of this persistent inoculum is also dependent of the antibiotic used. In our intracellular model, indeed, a larger maximal efficacy (more-negative  $E_{\text{max}}$ ) is obtained with moxifloxacin (as confirmed here) or with the highly bactericidal lipoglycopeptide oritavancin (21).

The pharmacodynamic model also shows that the intracellular forms of bacteria resistant to other antibiotics are almost uniformly susceptible to GSK1322322, with essentially similar  $C_s$  and  $E_{\text{max}}$  parameters across the whole range of strains examined. This extends to the intracellular forms of *S. aureus* what has been observed for extracellular bacteria concerning the lack of cross- or coreistance of this bacteria to GSK1322322 and other antibiotics in current clinical use. In contrast, strains that are resistant to the comparators show a markedly decreased relative potency (markedly increased  $C_s$ ) compared to the susceptible strains in proportion to their MIC differences in broth. Whether a maximal relative efficacy ( $E_{\text{max}}$ ) similar to that of the susceptible strain is reached or not depends essentially of the level of resistance. Thus, for strains with only a modest elevation of MIC, increasing the extracellular concentration allows overcoming the decreased susceptibility. This strongly suggests that the MIC actually drives both the extracellular response and intracellular response of the bacteria to the antibiotics. For strains with very large drug MICs where  $E_{\text{max}}$  remains positive, we simply were unable to increase the concentration to the necessary levels.

Pharmacokinetic studies suggest that GSK1322322 passively diffuses into and out of the cells, based on (i) the very similar and high rates of influx and efflux and the absence of saturation over the range of concentrations investigated (1 to 100 times the median MIC of GSK1322322), which collectively plead against the idea of carrier-mediated inward transport, and (ii) the impairment of drug movement by decreasing the temperature, which is consistent with lower diffusion through membrane bilayers when fluidity is considerably reduced. Accumulation of GSK1322322 was modest compared to that of other antibiotics such as macrolides and ketolides (35, 53, 54) and was more comparable to the range observed for fluoroquinolones (19, 41). It was not influenced by the addition of known inhibitors of multidrug efflux transporters in murine J774 macrophages. By and large, the pharmacokinetic behavior of GSK1322322 is therefore rather similar to that of moxifloxacin (fast accumulation and release; not a sub-



strate for active efflux in J774 macrophages; 41) even though the structures of the two compounds are totally unrelated.

The capacity of GSK1322322 to penetrate within eukaryotic cells contributes to rationalize the fact that it is active intracellularly. Yet cellular accumulation by itself is not a factor predictive of intracellular activity, since other drugs showing intracellular efficacy comparable to that of GSK1322322 displayed very different cellular-concentration-to-extracellular-concentration ratios in the same cellular model (spanning ~40-fold for azithromycin to ~4-fold for oxacillin and ~0.5-fold for linezolid) (21, 36). This conclusion was already reached in comparisons of drugs within the same pharmacological class, such as oxazolidinones (36), ketolides (35), and fluoroquinolones (18). The present report not only extends this concept to drugs of different pharmacological classes but also shows that it concerns drugs that are bacteriostatic as well as bactericidal toward extracellular bacteria. We have no simple explanation for this apparently counterintuitive conclusion, but we may suggest that the cellular accumulation of antibiotics actually reflects a reversible binding of part of the drug to cellular constituents, leaving only the free fraction (in equilibrium with the extracellular concentration) available for acting on the bacteria.

The results of the cell fractionation studies also bring some support for this concept. We see indeed that GSK1322322 accumulated by cells is never found in a stable association with subcellular organelles but is rather recovered in the fractions where soluble enzymes are also collected. This is observed even in infected cells where we see an almost complete dissociation between bacteria and the antibiotic. As the mode of action of GSK1322322 is that of a reversible binding to its bacterial target (55), we may propose that what the cell fractionation study reveals is the ability of the drug to freely diffuse into cells during the incubation but, thereafter, to be desorbed from it and be recovered in the supernatant of infected cells. The same proposal was made for fluoroquinolones, which also show no association with phagolysosomes after cell fractionation even though we know that they are very active against phagocytized bacteria (19, 21). Alternatively, one could propose that the small amounts of GSK1322322 observed in the fractions enriched in lysosomes could represent the active part of the antibiotic.

The present study had limitations related to the type of model used which have been discussed in previous publications. In the context of the present study, we must first mention our inability to take into account the binding of GSK1322322 to serum proteins (estimated to be <69% in humans on the basis of *in vitro* study results; 56) because the small (10%) amount of proteins in the cell culture medium made a large proportion of protein-bound drugs actually free, as demonstrated earlier for ertapenem (57), a highly

**FIG 7** Subcellular distribution of [<sup>14</sup>C]GSK1322322, marker enzymes (lactate dehydrogenase, cytosol; cytochrome *c*-oxidase, mitochondria; N-acetyl-β-hexosaminidase, lysosomes) and *S. aureus* (CFU) in homogenates of infected THP-1 monocytes. Cells were allowed to phagocytize opsonized *S. aureus* ATCC 25923 for 1 h at 37°C and were then returned to fresh medium for 2 h to allow complete internalization of bacteria, after which time they were exposed to 0.1 mg/liter [<sup>14</sup>C]GSK1322322 for 30 min, washed, homogenized, and fractionated as described for the experiment whose results are shown in Fig. 5 except that fractions ML and P were obtained as a single fraction (see the top of the graph for all fractions). The mode of representation is similar to that described for Fig. 5.

protein-bound  $\beta$ -lactam. Second, we limited our exposure times to 24 h, which prevented us from capturing earlier or later effects of the antibiotics on the intracellular bacteria. Third, we could not perform morphological observations of the subcellular disposition of GSK1322322 (which could have been useful as an alternative to the cell fractionation approach used) because of a lack of a suitable photonic tracer. Nevertheless, the present report as it stands demonstrates the ability of GSK1322322 to act as a typical PDF inhibitor of intracellular *S. aureus* strains that are both susceptible and resistant to several currently marketed antistaphylococcal antibiotics. It raises the issue of the apparent lack of correlation between cellular accumulation and disposition and the activity of antibiotics, which will need to be addressed in future experiments. Lastly, and while this work was being finalized, the clinical development of GSK1322322 was terminated (<https://www.clinicaltrials.gov/ct2/results?Search=Search>), illustrating the challenges of antibacterial development. However, the data from this study demonstrate some of the promising attributes of GSK1322322 and this class of antibiotics. This study could, therefore, be used as model for the assessment of other peptide deformylase inhibitors with respect to activity against intracellular forms of *S. aureus* and of other bacterial pathogens.

#### ACKNOWLEDGMENTS

We thank Gwenn Huys for help in some parts of this study and M. C. Cambier, K. Santos Saial, and P. Muller for dedicated technical assistance.

This work was supported in part by GlaxoSmithKline, Colledgeville, PA. Additional support was obtained from the Belgian Fonds de la Recherche Scientifique (grant 3.4530.12) and the Interuniversity Attraction Poles Program initiated by the Belgian Science Policy Office (program IAP P7/28).

#### REFERENCES

- Tarai B, Das P, Kumar D. 2013. Recurrent challenges for clinicians: emergence of methicillin-resistant *Staphylococcus aureus*, vancomycin resistance, and current treatment options. *J Lab Physicians* 5:71–78. <http://dx.doi.org/10.4103/0974-2727.119843>.
- Chung DR, Huh K. 2015. Novel pandemic influenza A (H1N1) and community-associated methicillin-resistant *Staphylococcus aureus* pneumonia. *Expert Rev Anti Infect Ther* 13:197–207. <http://dx.doi.org/10.1586/14787210.2015.999668>.
- Wolkewitz M, Frank U, Philips G, Schumacher M, Davey P. 2011. Mortality associated with in-hospital bacteraemia caused by *Staphylococcus aureus*: a multistate analysis with follow-up beyond hospital discharge. *J Antimicrob Chemother* 66:381–386. <http://dx.doi.org/10.1093/jac/dkq424>.
- Lowy FD. 2000. Is *Staphylococcus aureus* an intracellular pathogen? *Trends Microbiol* 8:341–343. [http://dx.doi.org/10.1016/S0966-842X\(00\)01803-5](http://dx.doi.org/10.1016/S0966-842X(00)01803-5).
- Sinha B, Herrmann M. 2005. Mechanism and consequences of invasion of endothelial cells by *Staphylococcus aureus*. *Thromb Haemostasis* 94:266–277.
- Sinha B, Fraunholz M. 2010. *Staphylococcus aureus* host cell invasion and post-invasion events. *Int J Med Microbiol* 300:170–175. <http://dx.doi.org/10.1016/j.ijmm.2009.08.019>.
- Wright JA, Nair SP. 2010. Interaction of staphylococci with bone. *Int J Med Microbiol* 300:193–204. <http://dx.doi.org/10.1016/j.ijmm.2009.10.003>.
- Clement S, Vaudaux P, Francois P, Schrenzel J, Huggler E, Kampf S, Chaponnier C, Lew D, Lacroix JS. 2005. Evidence of an intracellular reservoir in the nasal mucosa of patients with recurrent *Staphylococcus aureus* rhinosinusitis. *J Infect Dis* 192:1023–1028. <http://dx.doi.org/10.1086/432735>.
- Bosse MJ, Gruber HE, Ramp WK. 2005. Internalization of bacteria by osteoblasts in a patient with recurrent, long-term osteomyelitis. A case report. *J Bone Joint Surg Am* 87:1343–1347.
- Zautner AE, Krause M, Stropahl G, Holtfreter S, Frickmann H, Maletzki C, Kreikemeyer B, Pau HW, Podbielski A. 2010. Intracellular persisting *Staphylococcus aureus* is the major pathogen in recurrent tonsillitis. *PLoS One* 5:e9452. <http://dx.doi.org/10.1371/journal.pone.0009452>.
- Van Bambeke F, Barcia-Macay M, Lemaire S, Tulkens PM. 2006. Cellular pharmacodynamics and pharmacokinetics of antibiotics: current views and perspectives. *Curr Opin Drug Discov Devel* 9:218–230.
- Mazel D, Pochet S, Marliere P. 1994. Genetic characterization of polypeptide deformylase, a distinctive enzyme of eubacterial translation. *EMBO J* 13:914–923.
- Lewandowski T, Huang J, Fan F, Rogers S, Gentry D, Holland R, Demarsh P, Aubart K, Zalacain M. 2013. *Staphylococcus aureus* formylmethionyl transferase mutants demonstrate reduced virulence factor production and pathogenicity. *Antimicrob Agents Chemother* 57:2929–2936. <http://dx.doi.org/10.1128/AAC.00162-13>.
- Sutcliffe JA. 2011. Antibiotics in development targeting protein synthesis. *Ann N Y Acad Sci* 1241:122–152. <http://dx.doi.org/10.1111/j.1749-6632.2011.06323.x>.
- Chen DZ, Patel DV, Hackbarth CJ, Wang W, Dreyer G, Young DC, Demarsh PS, Wu C, Ni ZJ, Trias J, White RJ, Yuan Z. 2000. Actinonin, a naturally occurring antibacterial agent, is a potent deformylase inhibitor. *Biochemistry* 39:1256–1262. <http://dx.doi.org/10.1021/bi992245y>.
- O'Dwyer K, Hackel M, Hightower S, Hoban D, Bouchillon S, Qin D, Aubart K, Zalacain M, Butler D. 2013. Comparative analysis of the antibacterial activity of a novel peptide deformylase inhibitor, GSK1322322. *Antimicrob Agents Chemother* 57:2333–2342. <http://dx.doi.org/10.1128/AAC.02566-12>.
- Corey R, Naderer OJ, O'Riordan WD, Dumont E, Jones LS, Kurtinecz M, Zhu JZ. 2014. Safety, tolerability, and efficacy of GSK1322322 in the treatment of acute bacterial skin and skin structure infections. *Antimicrob Agents Chemother* 58:6518–6527. <http://dx.doi.org/10.1128/AAC.03360-14>.
- Vallet CM, Marquez B, Ngabirano E, Lemaire S, Mingeot-Leclercq MP, Tulkens PM, Van Bambeke F. 2011. Cellular accumulation of fluoroquinolones is not predictive of their intracellular activity: studies with gemifloxacin, moxifloxacin and ciprofloxacin in a pharmacokinetic/pharmacodynamic model of uninfected and infected macrophages. *Int J Antimicrob Agents* 38:249–256.
- Carlier MB, Scornameaux B, Zenebergh A, Desnottes JF, Tulkens PM. 1990. Cellular uptake, localization and activity of fluoroquinolones in uninfected and infected macrophages. *J Antimicrob Chemother* 26(Suppl B):27–39. [http://dx.doi.org/10.1093/jac/26.suppl\\_B.27](http://dx.doi.org/10.1093/jac/26.suppl_B.27).
- Seral C, Van Bambeke F, Tulkens PM. 2003. Quantitative analysis of gentamicin, azithromycin, telithromycin, ciprofloxacin, moxifloxacin, and oritavancin (LY333328) activities against intracellular *Staphylococcus aureus* in mouse J774 macrophages. *Antimicrob Agents Chemother* 47:2283–2292. <http://dx.doi.org/10.1128/AAC.47.7.2283-2292.2003>.
- Barcia-Macay M, Seral C, Mingeot-Leclercq MP, Tulkens PM, Van Bambeke F. 2006. Pharmacodynamic evaluation of the intracellular activities of antibiotics against *Staphylococcus aureus* in a model of THP-1 macrophages. *Antimicrob Agents Chemother* 50:841–851. <http://dx.doi.org/10.1128/AAC.50.3.841-851.2006>.
- Peyrusson F, Huys G, Van Bambeke F, Butler G, Tulkens PM. 2014. Abstr 54th Intersci Conf Antimicrob Agents Chemother [ICAAC], Washington, DC, 5 to 9 September 2014, poster A-686.
- Peyrusson F, Tulkens PM, Van Bambeke F. 2014. Abstr 24th Eur Congr Clin Microbiol Infect Dis [ECCMID], Barcelona, Spain, 10 to 13 May 2014, electronic poster eP185 with oral presentation.
- Tsuchiya S, Yamabe M, Yamaguchi Y, Kobayashi Y, Konno T, Tada K. 1980. Establishment and characterization of a human acute monocytic leukemia cell line (THP-1). *Int J Cancer* 26:171–176. <http://dx.doi.org/10.1002/ijc.2910260208>.
- Snyderman R, Pike MC, Fischer DG, Koren HS. 1977. Biologic and biochemical activities of continuous macrophage cell lines P388D1 and J774.1. *J Immunol* 119:2060–2066.
- Renard C, Vanderhaeghe HJ, Claes PJ, Zenebergh A, Tulkens PM. 1987. Influence of conversion of penicillin G into a basic derivative on its accumulation and subcellular localization in cultured macrophages. *Antimicrob Agents Chemother* 31:410–416. <http://dx.doi.org/10.1128/AAC.31.3.410>.
- Scornameaux B, Ouadrhiri Y, Anzalone G, Tulkens PM. 1996. Effect of recombinant human gamma interferon on intracellular activities of antibiotics against *Listeria monocytogenes* in the human macrophage cell line THP-1. *Antimicrob Agents Chemother* 40:1225–1230.

28. Kosowska-Shick K, Clark C, Credito K, McGhee P, Dewasse B, Bogdanovich T, Appelbaum PC. 2006. Single- and multistep resistance selection studies on the activity of retapamulin compared to other agents against *Staphylococcus aureus* and *Streptococcus pyogenes*. *Antimicrob Agents Chemother* 50:765–769. <http://dx.doi.org/10.1128/AAC.50.2.765-769.2006>.
29. Tsiodras S, Gold HS, Sakoulas G, Eliopoulos GM, Wennersten C, Venkataraman L, Moellering RC, Ferraro MJ. 2001. Linezolid resistance in a clinical isolate of *Staphylococcus aureus*. *Lancet* 358:207–208. [http://dx.doi.org/10.1016/S0140-6736\(01\)05410-1](http://dx.doi.org/10.1016/S0140-6736(01)05410-1).
30. Baudoux P, Lemaire S, Denis O, Tulkens PM, Van Bambeke F, Glupczynski Y. 2010. Activity of quinupristin/dalfopristin against extracellular and intracellular *Staphylococcus aureus* with various resistance phenotypes. *J Antimicrob Chemother* 65:1228–1236. <http://dx.doi.org/10.1093/jac/dkq110>.
31. European Committee on Antimicrobial Susceptibility Testing. 2015. Breakpoint tables for interpretation of MICs and zone diameters (version 5.0). European Committee on Antimicrobial Susceptibility Testing. <http://www.eucast.org>. Last updated, 26 January 2015; last accessed, 30 January 2015.
32. Clinical and Laboratory Standards Institute. 2014. Performance standards for antimicrobial susceptibility testing; 24th informational supplement (M5100-S24). Clinical and Laboratory Standards Institute, Wayne, PA.
33. Lemaire S, Kosowska-Shick K, Appelbaum PC, Glupczynski Y, Van Bambeke F, Tulkens PM. 2011. Activity of moxifloxacin against intracellular community-acquired methicillin-resistant *Staphylococcus aureus*: comparison with clindamycin, linezolid and co-trimoxazole and attempt at defining an intracellular susceptibility breakpoint. *J Antimicrob Chemother* 66:596–607. <http://dx.doi.org/10.1093/jac/dkq478>.
34. Buyck J, Lemaire S, Seral C, Anantharajah A, Peyrusson F, Tulkens PM, Van Bambeke F. 2015. In vitro models for the study of the intracellular activity of antibiotics, p 147–157. In Michiels J, Fauvart M (ed), *Bacterial persistence (Molecular Biology Laboratory Protocols Series)*. Humana Press (Springer), New York, NY.
35. Lemaire S, Van Bambeke F, Tulkens PM. 2009. Cellular accumulation and pharmacodynamic evaluation of the intracellular activity of CEM-101, a novel fluoroketolide, against *Staphylococcus aureus*, *Listeria monocytogenes*, and *Legionella pneumophila* in human THP-1 macrophages. *Antimicrob Agents Chemother* 53:3734–3743. <http://dx.doi.org/10.1128/AAC.00203-09>.
36. Lemaire S, Van Bambeke F, Appelbaum PC, Tulkens PM. 2009. Cellular pharmacokinetics and intracellular activity of torezolid (TR-700): studies with human macrophage (THP-1) and endothelial (HUVEC) cell lines. *J Antimicrob Chemother* 64:1035–1043. <http://dx.doi.org/10.1093/jac/dkp267>.
37. Lemaire S, Glupczynski Y, Duval V, Joris B, Tulkens PM, Van Bambeke F. 2009. Activities of ceftobiprole and other cephalosporins against extracellular and intracellular (THP-1 macrophages and keratinocytes) forms of methicillin-susceptible and methicillin-resistant *Staphylococcus aureus*. *Antimicrob Agents Chemother* 53:2289–2297. <http://dx.doi.org/10.1128/AAC.01135-08>.
38. Mélard A, Garcia LG, Das D, Rozenberg R, Tulkens PM, Van Bambeke F, Lemaire S. 2013. Activity of ceftaroline against extracellular (broth) and intracellular (THP-1 monocytes) forms of methicillin-resistant *Staphylococcus aureus*: comparison with vancomycin, linezolid and daptomycin. *J Antimicrob Chemother* 68:648–658. <http://dx.doi.org/10.1093/jac/dks442>.
39. Seral C, Michot JM, Chanteux H, Mingeot-Leclercq MP, Tulkens PM, Van Bambeke F. 2003. Influence of p-glycoprotein inhibitors on accumulation of macrolides in j774 murine macrophages. *Antimicrob Agents Chemother* 47:1047–1051. <http://dx.doi.org/10.1128/AAC.47.3.1047-1051.2003>.
40. Van Bambeke F, Carryn S, Seral C, Chanteux H, Tyteca D, Mingeot-Leclercq MP, Tulkens PM. 2004. Cellular pharmacokinetics and pharmacodynamics of the glycopeptide antibiotic oritavancin (LY333328) in a model of J774 mouse macrophages. *Antimicrob Agents Chemother* 48:2853–2860. <http://dx.doi.org/10.1128/AAC.48.8.2853-2860.2004>.
41. Michot JM, Seral C, Van Bambeke F, Mingeot-Leclercq MP, Tulkens PM. 2005. Influence of efflux transporters on the accumulation and efflux of four quinolones (ciprofloxacin, levofloxacin, garenoxacin, and moxifloxacin) in J774 macrophages. *Antimicrob Agents Chemother* 49:2429–2437. <http://dx.doi.org/10.1128/AAC.49.6.2429-2437.2005>.
42. Lowry OH, Rosebrough NJ, Farr AL, Randall RJ. 1951. Protein measurement with the Folin phenol reagent. *J Biol Chem* 193:265–275.
43. Lemaire S, Tulkens PM, Van Bambeke F. 2010. Cellular pharmacokinetics of the novel biaryloxazolidinone radezolid in phagocytic cells: studies with macrophages and polymorphonuclear neutrophils. *Antimicrob Agents Chemother* 54:2540–2548. <http://dx.doi.org/10.1128/AAC.01723-09>.
44. Flanagan S, McKee EE, Das D, Tulkens PM, Hosako H, Fiedler-Kelly J, Passarell J, Radovsky A, Prokocimer P. 2015. Nonclinical and pharmacokinetic assessments to evaluate the potential of tedizolid and linezolid to affect mitochondrial function. *Antimicrob Agents Chemother* 59:178–185. <http://dx.doi.org/10.1128/AAC.03684-14>.
45. Baudoux P, Bles N, Lemaire S, Mingeot-Leclercq MP, Tulkens PM, Van Bambeke F. 2007. Combined effect of pH and concentration on the activities of gentamicin and oxacillin against *Staphylococcus aureus* in pharmacodynamic models of extracellular and intracellular infections. *J Antimicrob Chemother* 59:246–253.
46. Lemaire S, Van Bambeke F, Pierard D, Appelbaum PC, Tulkens PM. 2011. Activity of fusidic acid against extracellular and intracellular *Staphylococcus aureus*: influence of pH and comparison with linezolid and clindamycin. *Clin Infect Dis* 52(Suppl 7):S493–S503. <http://dx.doi.org/10.1093/cid/cir165>.
47. Lemaire S, Van Bambeke F, Mingeot-Leclercq MP, Glupczynski Y, Tulkens PM. 2007. Role of acidic pH in the susceptibility of intraphagocytic methicillin-resistant *Staphylococcus aureus* strains to meropenem and cloxacillin. *Antimicrob Agents Chemother* 51:1627–1632. <http://dx.doi.org/10.1128/AAC.01192-06>.
48. Sandberg A, Jensen KS, Baudoux P, Van Bambeke F, Tulkens PM, Fridtjof-Nielsen N. 2010. Intra- and extracellular activities of dicloxacillin against *Staphylococcus aureus* in vivo and in vitro. *Antimicrob Agents Chemother* 54:2391–2400. <http://dx.doi.org/10.1128/AAC.01400-09>.
49. Sandberg A, Jensen KS, Baudoux P, Van Bambeke F, Tulkens PM, Fridtjof-Nielsen N. 2010. Intra- and extracellular activity of linezolid against *Staphylococcus aureus* in vivo and in vitro. *J Antimicrob Chemother* 65:962–973. <http://dx.doi.org/10.1093/jac/dkq052>.
50. Bauer J, Siala W, Tulkens PM, Van Bambeke F. 2013. A combined pharmacodynamic quantitative and qualitative model reveals the potent activity of daptomycin and delafloxacin against *Staphylococcus aureus* biofilms. *Antimicrob Agents Chemother* 57:2726–2737. <http://dx.doi.org/10.1128/AAC.00181-13>.
51. Lechner S, Lewis K, Bertram R. 2012. *Staphylococcus aureus* persists tolerant to bactericidal antibiotics. *J Mol Microbiol Biotechnol* 22:235–244. <http://dx.doi.org/10.1159/000342449>.
52. Singh R, Ray P, Das A, Sharma M. 2009. Role of persisters and small-colony variants in antibiotic resistance of planktonic and biofilm-associated *Staphylococcus aureus*: an in vitro study. *J Med Microbiol* 58:1067–1073. <http://dx.doi.org/10.1099/jmm.0.009720-0>.
53. Carlier MB, Zenebergh A, Tulkens PM. 1987. Cellular uptake and subcellular distribution of roxithromycin and erythromycin in phagocytic cells. *J Antimicrob Chemother* 20(Suppl B):47–56. [http://dx.doi.org/10.1093/jac/20.suppl\\_B.47](http://dx.doi.org/10.1093/jac/20.suppl_B.47).
54. Carlier MB, Garcia-Luque I, Montenez JP, Tulkens PM, Piret J. 1994. Accumulation, release and subcellular localization of azithromycin in phagocytic and non-phagocytic cells in culture. *Int J Tissue React* 16:211–220.
55. Sangshetti JN, Khan FAK, Shinde DB. 2015. Peptide deformylase: a new target in antibacterial, antimalarial and anticancer drug discovery. *Curr Med Chem* 22:214–236.
56. Naderer OJ, Dumont E, Zhu J, Kurtinecz M, Jones LS. 2013. Single-dose safety, tolerability, and pharmacokinetics of the antibiotic GSK1322322, a novel peptide deformylase inhibitor. *Antimicrob Agents Chemother* 57:2005–2009. <http://dx.doi.org/10.1128/AAC.01779-12>.
57. Lemaire S, Van Bambeke F, Mingeot-Leclercq MP, Tulkens PM. 2005. Activity of three  $\beta$ -lactams (ertapenem, meropenem and ampicillin) against intraphagocytic *Listeria monocytogenes* and *Staphylococcus aureus*. *J Antimicrob Chemother* 55:897–904. <http://dx.doi.org/10.1093/jac/dki094>.